Effect of the Radial Constrain for the Impact Energy-Absorbing Behaviour of the Closed-Cell Metal Foam

József Kertész[1,2(✉)] and Tünde Anna Kovács[3]

[1] School on Safety and Security Sciences, Óbuda University, Budapest 1081, Hungary
kertesz.jozsef@eng.unideb.hu
[2] Air- and Road Vehicle Department, University of Debrecen, Debrecen, Hungary
[3] Donát Bánki Faculty of Mechanical and Safety Engineering, Óbuda University, Budapest 1081, Hungary

Abstract. The application of metal foam in the vehicle industry is not a novelty. Owing to the strict emission and consumption requirements, the use of composites and metal foams can be useful for reducing the mass for car manufacturers. Along with sustainability, higher safety features are also expected by the users in the case of new vehicles. This requirement also confirms the necessity of the metal foam application in the vehicle structure since the porous feature results in high absorbed energy by the low mass. The present study is a prework of subsequent development of a special crumple Crushbox part of the vehicle front, which is working on the principle of radial constrained foam compression. In this study discussed compression experiments confirm the fact, that the energy absorbed capacity of a metal foam can be improved in different radial constrained applications. The significant absorbed energy difference can be expected due to the increase in the densification region.

Keywords: Constrain · Aluminium-foam · Impact · Energy-absorption

1 Introduction

Many recent investigations are about the metal foam application in vehicle body parts. All of them report the positive effect of the metal foam application in the case of energy-absorbing capacity. [1–5] The typical investigation of the metal foams to reviled the physical properties, the compression test. In the practice, we have many options for manufacturing metal foam, furthermore, the different manufacturing process results in different material properties in the end-product. [6–8] However to get real appreciable and comparable results with the compression test, it is mandatory to provide the conditions and the requirements the standard expects. In the case of the applied compression test to the reveal of the mechanical properties of a metal foam the ISO13314:2011: Compression test for porous and cellular metals, and the ISO17340:2020: High speed compression test for porous and cellular metals must be taken into consideration. [9, 10] The experiments about the mechanical properties of the metal foam can be dived

into two groups. According to this, we can distinguish quasi-static and dynamic compression tests. In the case of the first, the main aim of it is to analyse the full length of the stress-and strain diagram of the compression test and concludes the possibilities of the application and its later development of it. [11–13] However the dynamic test is focusing on the energy absorbed capacity most of all. Both compression experiment results in special stress-and strain character, which has three main typical parts. Helping with these parts the foam's features can be compared purely. All of the type of foam (opened-cell, closed-cell, syntactic-foam) has the main features under compression test. Our investigation focuses on closed-cell aluminium foam. Lightweight aluminium alloy closed-cell foams are one of the most important classes of cellular materials for structural applications. They have frequently been applied as a core of sandwich panels [14] or a filler material [15] of hollow structures (Crushbox) for several multi-functional construction elements in vehicles as crash energy, sound and vibration absorption. When an object is moving it has kinetic energy, and the amount of it is influenced by the amount of its mass and the velocity. At the moment of the impact, the previous mentioned kinetic energy is converted into impact energy. The vehicle safety crumple zone aims to absorb the most impact energy to reduce the effect of the impact force that would load the passengers. The impact absorbing capacity of the vehicle can be improved from the side of shape or applied-material optimisation. Our investigation is about the absorbing improvement with the application of aluminium foam. A compression load of the foams results in three segmented stress-strain diagrams. Our aim is the maximum utilisation of the plateau region and the incipient densification state for energy absorption. At the beginning of the research, we started with the hypothesis that if we can influence the steepness and shape of the stress-strain diagram of given metal foam with a design solution, we can influence the amount of energy it can absorb. Owing to this assumption, we apply a tube around the foam specimen to hinder its radial displacement of it. The literature describes this construction with the "radial constrained compression" expression. When the constraining tube inner diameter is equal to the initial outer diameter of the foam specimen it is the radial constrained structure. Tons of investigation is about the free compression test of aluminium foams with quasi-static load, but the field of the constrained examines with dynamics load are less. However, these reports have good results in the case of absorbing the energy effect. Li et al. share their study that the performance of the foam absorbing energy per unit volume can be greatly improved by the radial constraints. [16] In the present study, we would like to reveal and prove the impact energy absorbing improvement effect of the applied constraining tubes. Therefore, we have taken a comparison examination, where the same aluminium foam was compressed in three different ways. The first case was about free compression, the second one was about radial constrained compression. Figure 1 represents the set of the different specimen construction.
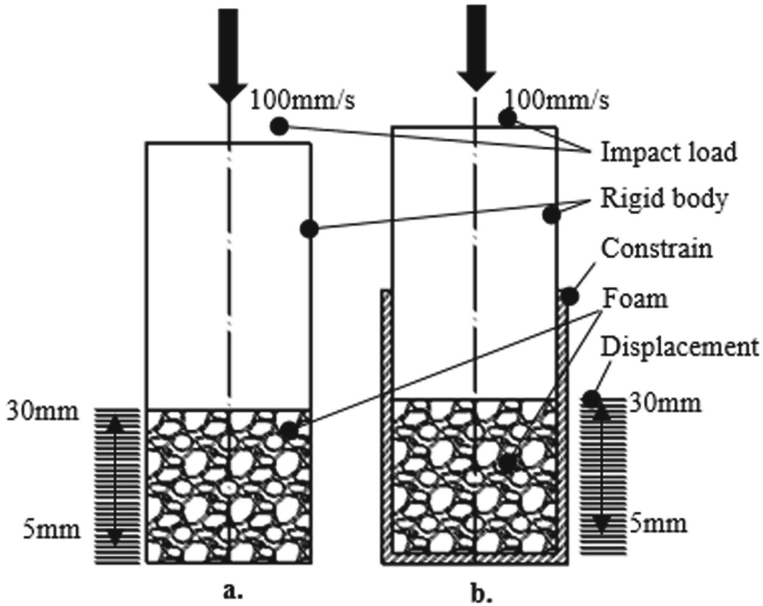
Fig. 1. The set of the specimens **a.** Free compression **b.** Radial constrained compression [author]

2   Material and Experimental Methods

For the comparison test, we applied cylindrical specimens taking into consideration the requirement of the ISO13314 and ISO17340 standards. The diameter and the length of the foam were chosen for 30 mm. For the radial constrained compressing we used a 30 mm inner diameter and 50 mm length cylindrical ended-tube with a 2 mm wall made from AlMgSi1. The foam is a closed-cell aluminium foam with an average 0,3 g/cm3 density. The exact material ingredients of the foam are not detailed in this study, since the aim is to focus on the structure effect and not the material examination. From this point of view, the applied foam type is independent of the comparison test. For the constrained test we applied a rigid cylindrical body made from steel with 30 mm diameter and 50 mm length.

2.1   Experimental Methods and Technology

The tests were performed on an Instron 8801 servo-hydraulic material testing machine. This system is suitable for static and dynamic material testing due to its rigid frame design. The research aims to develop a high-efficiency impact energy-absorbing body element, the effectiveness of which I base on the radially inhibited compaction of metal foams. In an accident, the structure is subjected to a dynamic load due to a collision. Therefore, we perform the tests according to the guidelines of the ISO17340: 2020 standard. This standard specifies boundary conditions for high-speed compaction testing of porous materials. A dynamic test is when the compaction speed is at least 0.1 m/s. This standard sets the upper-speed limit at 100 m/s. Accordingly, the test was performed at a

compaction speed of 100 mm/s. An Instron 8800MiniTower control unit is used to control the Istron 8801 material testing system. To record the measurement boundary conditions and data, the computer is connected to the control unit via an interface cable. The software required to use the system is the WaveMatrix software package. The purpose of the measurement is to record the response properties of the metal foam to its compaction, i.e. to record the engineering stress-strain diagram and to evaluate them. Instron® it is the only manufacturer that develops and manufactures the transmitters and sensors required for the measurements itself, so we use an Instron 149464 100 kN force-measuring cell for the measurements so that we can record the most authentic data. The safety and calibration requirements specified by the manufacturer have also been taken into account in the design and performance of the measurement, as current standards recommend that the interval between calibrations should not exceed 18 months. The measuring system met this requirement. After many empty test-run, we found that the correct data recording must be used a minimum of 125 mm displacement for the test. In which the first 100 mm is for the acceleration of the crosshead of the machine to reach the 0,1 m/s speed, and the rest 25 mm is the compression of the foam. For this displacement, we can reach the 80% strain to get an evaluable result. To get representative results, we repeat every compression test three times. Figure 2 shows the set of the measuring device.

Fig. 2. Instron 8801 prepared for the compression test [author]

3   Interpretation of the Stress-Strain Diagram

To compare the effect of the different construction filled with aluminium foam, a standardised interpretation is necessary. In the next, the definitions are defined according to

the above mentioned ISO standards. In the case of porous and cellular material compression, the compressive stress can be determined with the compressive force divided by the initial cross-section. The horizontal (y-axis) of the diagram indicates the strain, which can be calculated by the proportion of the actual displacement and the initial length of the specimen. We compared the first maximum compressive stress values, so the definition of it is important. In this case, the first local maximum can correspond with the maximum compressive stress. The study focuses on the amount of absorbed energy, so the interpretation of the plateau stress cannot be neglected. The plateau is the arithmetical mean of the stresses between 20% and 40% compressive strain. The results of this region are the base of the calculation of the densification strain point. The end of the plateau and the start of the densification region can correspond with the 1,3 times the plateau stress. Finally, we calculate the absorbed energy in two different ways. First – as the standard also suggests – the energy is the area under the stress-strain curve up to 50% strain or up to the plateau end strain. After it, we calculate the area under the curve up to 80% strain, a significant difference is expected in the densification region due to radial constrain. Figure 3 Represents the typical stress-strain diagram of foam compression. For the area calculation under the curve, we use the integration with the trapezoidal rule, according to the next formula:

$$\int_0^{0.5-0.8} \frac{f(x)dx \approx}{\frac{1}{2}\sum_{i=1}^{N}(f(x_i)+f(x_{i+1}))(x_{i+1}-x_i)} \tag{1}$$
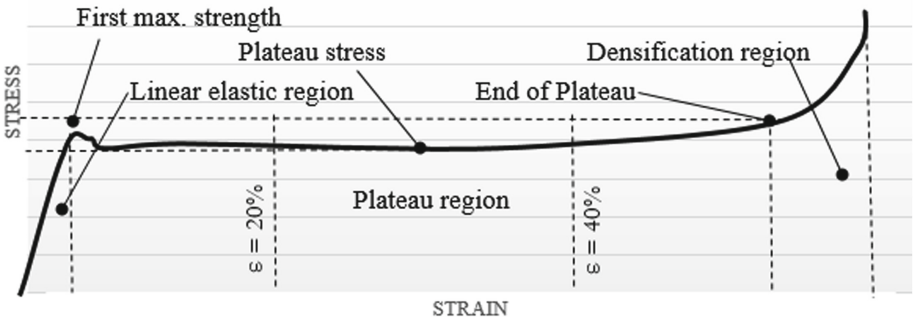

Fig. 3. Typical stress-strain diagram of the aluminium foam compression [author]

4   Specimen Preparation

To avoid the influence of the inner material structural deviation, before the compression we recorded the exact geometry parameters and weight of the specimens. For all tests we use the same nominal size specimens, however, owing to the uneven cellular distribution the density definition is important. We performed three free-compression, three radial constrained compression tests, and all of them are repeated by three times, resulting in six pieces' specimens. The parameters of the specimens are collected in Table 1.

Table 1. Parameters of the specimens [author]

No.	D [mm]	L [mm]	m [g]	ρ [g/cm3]
SP1	29.77	29.61	6.98	0.30
SP2	29.88	29.35	6.94	0.29
SP3	29.91	30.17	6.85	0.29
SP4	29.89	30.13	7.51	0.32
SP5	29.84	30.12	6.96	0.30
SP6	29.82	30.02	7.97	0.34
Avge	29.85	29.89	7.19	0.30

Table 1 confirms the specimen's geometry so the density tolerances are under 1%. The specimens from SP1-SP3 are examined with free-, the SP4-SP6 radial constrained.

5   Results of the Tests

5.1   Compression Test Without Constrain

In the first, we analysed the SP1–2-3 specimens, without any radial constraining. The results are reported in Table 2. All of the specimens resulted in the typical stress-strain diagram. The average of the plateau stress is 2.81 MPa was calculated in 20–40% strain range with 3.66 MPa plateau-end stress. The plateau reaches its end at the 50% strain. To analyse the effect of the constrain - in the next - for the plateau region we calculated the absorbed energy up to the beginning of the densification range. Considering the absorbed energy under compression, the significant (more than 80%) part of the whole was performed after the end of the plateau, in the densification range. Numerically up to 60% strain the foam absorbed 1.89 J, however up to 80% the energy was 11.17 J. The absorbed energy density has also an important function in the case of analysing the foam behaviour, therefore we have to define the amount of energy related to the volume. According to this, it has 2104.7 kJ/m3. The manufacturers frequently supply production descriptions; which manual contains normative information about the absorbed energy density related to each type of product [17]. Our specimens have an average 0.3 g/cm3 density means 2000 kJ/m3 energy density according to the product guide. It results in less than 10% difference between the real test and the literature data. The first maximum compression test was an average of 3.66 MPa. After the compression, we measured the diameter of the broken specimens, which was an average of 34.33 mm. Figure 4 shows the specimen before and after the impact load.
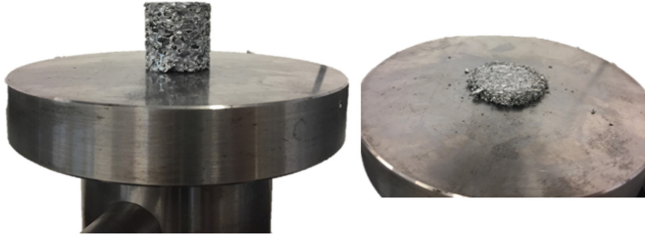
Fig. 4. Specimen before and after the free compression [author]

Figure 5–6 show the occurred stress-strain diagram about the free compression. Figure 5 indicates the compression until 60% strain, and then the full test is shown (until 80% strain). There are many recent studies in which the foam density and the compression behaviour were observed [18, 19]. These studies confirm the correctness of the earned results since they report the same values and results with 0.3 g/cm3 foam density. In Fig. 7 the steps of the compression can be seen at 0–30-50–80% strain.

Table 2. Results of the compression of the SP1–2-3 specimen without constrain [author]

	SP1	SP2	SP3	Avge	
σ_{pl}	2.95	2.89	2.62	2.82	MPa
$\sigma_{pl\ end}$	3.84	3.75	3.41	3.66	MPa
$\varepsilon_{pl\ end}$	51.76	50.76	47.51	50.01	%
$\sigma_{first\ max}$	3.03	2.81	2.60	2.81	MPa
$E_{abs.60}$	1.89	1.14	1.278	1.16	J
$E_{abs.80}$	11.18	11.42	11.39	11.39	J
Eabs. up to dens	1.45	0.66	0.50	0.59	J
Eabs. in the dens	10.72	10.77	10.90	10.80	J
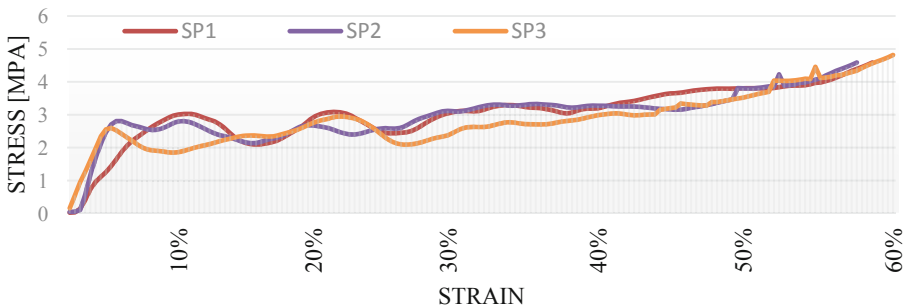
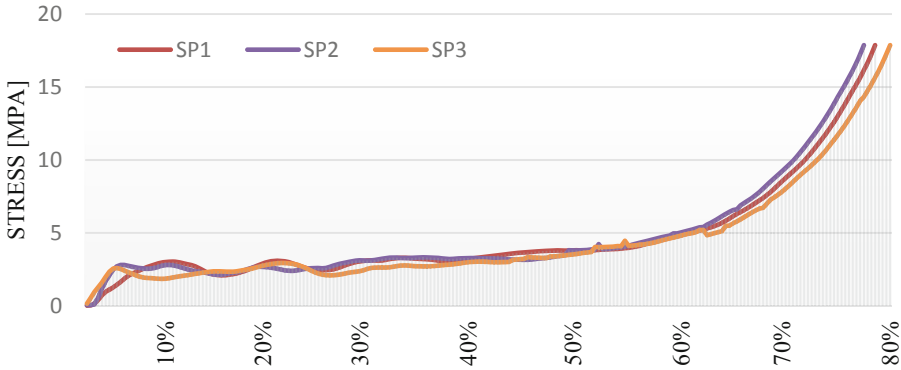**Fig. 5.** Compression without constrain (up to 60% strain) [author]

Fig. 6. Compression without constrain (up to 80% strain) [author]


Fig. 7. The steps of the free compression of the foam (0–30-50–80% strain) [author]

5.2 Compression Test with Radial-Constrain

In this section, the results of the radial constrained compression tests will be reported. As in the previous two test, the foam has the same mechanical behaviour in the linear-elastic range. The maximum compression strength was 5.434 MPa. The indicated plateau stress reaches 4.183 MPa. The significant difference began to appear in the second stage of the plateau range and the densification period. The stress-strain character was even steeper, and there is a remarkable increase in the second plateau region resulting in a higher amount of absorbed energy. The effect of the tube constrain was felt, since the radial displacement of the cells was constrained, and the hardening effect appeared already at the 44% strain. Figure 8 shows the state of the specimen before and after the impact load.

As a result of constraining the absorbed energy was 24.53 J. It means that the impact energy capacity was doubled only because of the application of the radial constrain related to the free compression. A significant part of this energy was absorbed naturally in the second half of the compression because of the hardening effect. Table 3 sums up the indicated results of the constrained test. As can be seen in Fig. 9–10. From the second half of the plateau region, the curve has notable steeper characteristics owing to the hardening effect.
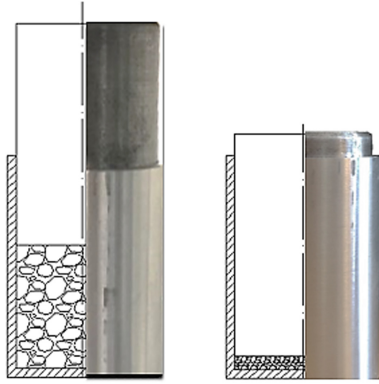
Fig. 8. Specimen before and after the collision load in half section by 2D/photo view [author]

Table 3. Results of the compression of the SP4–5-6 specimen with radial-constrain [author]

	SP4	SP5	SP6	Avge	
σ_{pl}	3.96	4.48	4.11	4.18	MPa
$\sigma_{pl\ end}$	5.16	5.82	5.34	5.44	MPa
$\varepsilon_{pl\ end}$	44.83	44.07	43.21	44.03	%
$\sigma_{first\ max}$	3.29	3.52	3.51	3.43	MPa
$E_{abs.60}$	3.78	3.86	3.68	3.77	J
$E_{abs.80}$	23.17	28.11	22.34	24.53	J
Eabs. up to dens	1.62	1.37	1.43	1.47	J
Eabs. in the dens	21.55	26.74	20.91	23.06	J
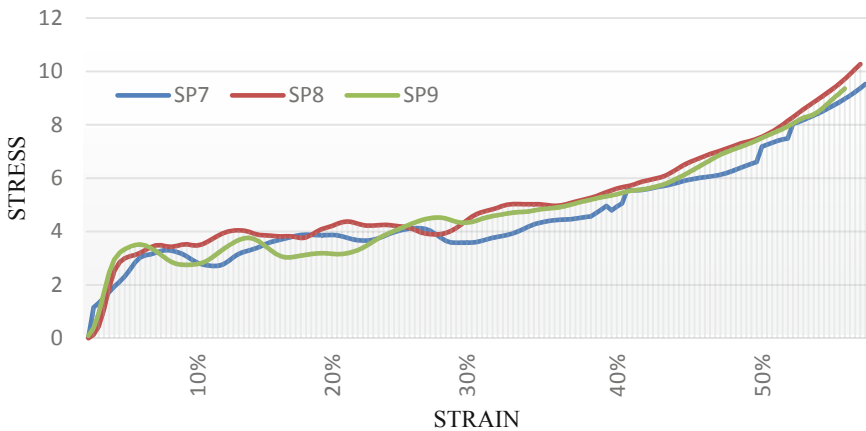
Fig. 9. Compression with radial constrain (up to 60% strain) [author]
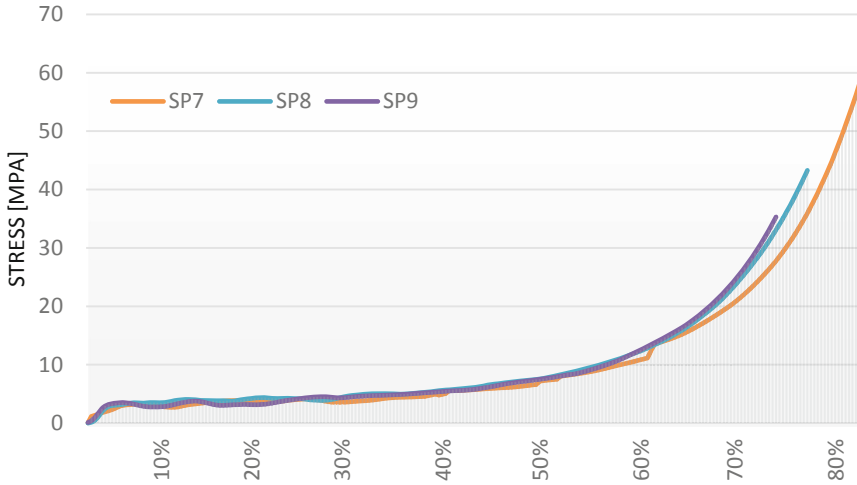
Fig. 10. Compression with radial constrain (up to 80% strain) [author]

6 Comparison of the Results

Figure 11 and Fig. 12 contain the two types of compression test in one diagram. In this diagram, the effect of the constrain is very spectacular. In the first elastic region, there is no significant difference, the curve has a similar steep shape, and this similarity stays till the half of the plateau region. However, after half of the plateau, the curves begin to separate. The hatched area indicates the absorbed energy difference. In the case of free compression, the foam was able to absorb an average of 11.391 J. However this value achieved the 22.342 J. It confirms that it can be achieved more effective energy absorbing with the application of a constrain with the same foam.
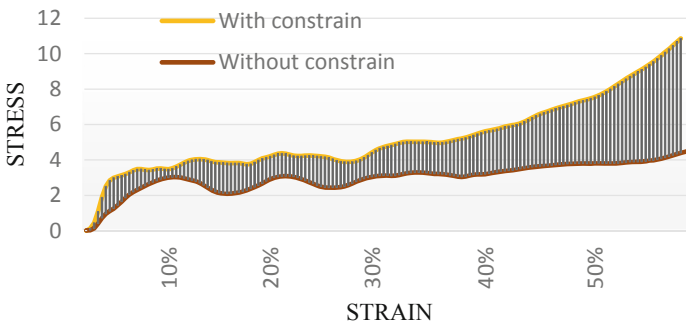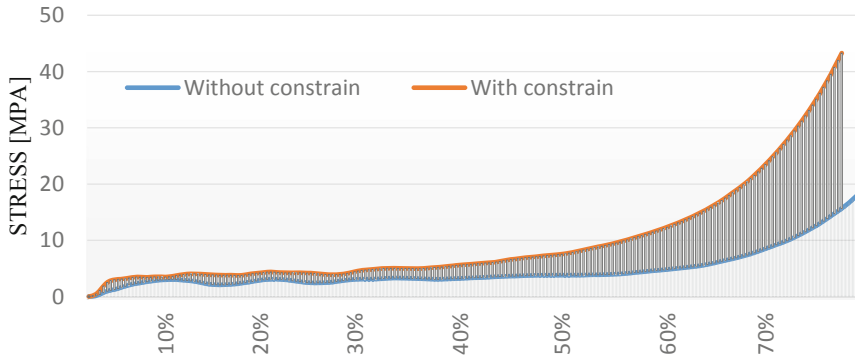

Fig. 11. Absorbed energy difference between the free and constrained test (up to 60% strain) [author]

Fig. 12. Absorbed energy difference between the free and constrained test (up to 80% strain) [author]

7   Conclusion

In this study, the effect of the radial constrain was observed in the case of closed-cell aluminium foam compression. The test was a prework of a latter crushbox optimisation, owing to this the investigation was focused on the absorbed energy performance. According to our prediction, the radial constrain can improve the energy absorbing capacity of the same foam. There was little difference in the linear elastic region; in all set up the specimens resulted in same behaviour. The constrain began to take effect in the second half of the plateau region significantly. The hardening effect was existed earlier with radial constrain, and the plateau line had remarkable steep. Due to the steeper characteristic, the absorbing energy in the plateau stage was higher than without constrain. The improved stress-strain character involved a higher amount of absorbed energy. The significant difference is recorded in the densification region. With radial constrain the character can be lifted remarkably. Considering the absorbed energy, it could be double with the constrain. Furthermore, it can be clearly stated from the measurement that the hardening behaviour (involving the energy absorbing) of metal foams can be influenced by the extent of radial constrain. The aim of the long-term investigation is to develop a vehicle crumple zone crushbox that is suited for more impact energy. We would like to divide the crushbox into more stage and fill it up with different mechanical featured foams and it will work on the principle of the radial constrained foam compression. This study confirms the fact, that with an optimised crumple structure, the impact energy absorbing performance can be improved in the case of the same featured foams. In the shadow of these results, we can start the structure developing and designing. Furthermore, since the constrain is not directly compressed in the impact, the material of it can be replaced by a lighter one which can also contribute to the mass optimisation of vehicles.

References

1. Joshi, S.Y., Kolhe, V.A.: Investigation on energy absorption properties of Al-foam, foam filled and empty MS tube under 3-point loading condition at room temperature. IOP Conf. Ser.: Mater. Sci. Eng. **409**(1), 012033, (2018)
2. Kolhe, V.A., Baviskar, P.R., Patil, M.M.: Bending characteristics of foam filled mild steel bumper beam under gradual loading condition. Int. J. Applied Eng. Res. ISSN 0973–4562 **13**(5), 64–68 (2018)
3. Yousefi, M.K., Kianirad, A., Vaseghi, M.: Simulation and investigation to the behavior of metallic foam as a bumper in automobile under impact loadings. The First International Conference on Mechanics of Advanced Materials and Equipment (2018)
4. Pandey, R., Singh, P., Khanna, M., Murtaza, Q.: Metal foam manufacturing, mechanical properties and its designing aspects—a review. Advances in Manufacturing and Industrial Engineering, pp. 761–770 (2021)
5. Marx, J., Rabiei, A.: Tensile properties of composite metal foam and composite metal foam core sandwich panels. J. Sandwich Structures and Materials **23**(8) 3773–3793 (2021). https://doi.org/10.1177/1099636220942880
6. Gyöngyösi, S., Gábora, A., Balogh, G., Kalácska, G., Bubonyi, T., Mankovits, T.: Effects of additives on the mechanical properties of aluminum foams. Mechanisms Machine Sci. **109,** 307–313. Paper: Chapter 28 , 7 p. (2022)
7. Kim, S., Lee, C.-W.: A review on manufacturing and application of open-cell metal foam. 8th International Conference on Porous Metals and Metallic Foams, Metfoam 2013, Procedia Materials Science **4**, 305–309 (2014)
8. Kulshreshtha, A., Dhakad, S.K.: Preparation of metal foam by different methods: a review. Materials Today: Proceedings **26** 1784–1790 (2020)
9. ISO 13314:2011 Mechanical testing of metals — Ductility testing — Compression test for porous and cellular metals
10. ISO 17340:2020 Metallic materials — Ductility testing — High speed compression test for porous and cellular metals
11. Kader, M.A., et al.: Macro and micro collapse mechanisms of closed-cell aluminium foams during quasi-static compression. Materials and Design **118**, 11–21 (2017)
12. Seitzberger, M., Rammerstorfer, F.G., Gradinger, R., Degischer, H.P., Blaimscheind, M., Walchd, C.: Experimental studies on the quasi-static axial crushing of steel columns filled with aluminium foam. Int. J. Solids Structures **37**, 4125–4147 (2000)
13. Mankovits, T., et al.: Structural analysis and its statistical evaluation of a closed-cell metal foam. Int. Review of Applied Sciences Eng. **5**(2), 135-143 (2014)
14. Radford, D.D., Deshpande, V.S., Fleck, N.A.: The use of metal foam projectiles to simulate shock loading on a structure. Int. J. Impact Eng. **31**(9), 1152–1171 (2005)
15. Duarte, I., Krstulovic-Opara, L., Vesenjak, M.: Characterisation of aluminium alloy tubes filled with aluminium alloy integral-skin foam under axial compressive loads. Composite Structures **121**, 154–162 (2015)
16. Li, C., Li, C., Wang, Y.: Compressive behavior and energy absorption capacity of unconstrained and constrained open-cell aluminum foams. Advanced Composites Letters **29**, 1–4 (2020). https://doi.org/10.1177/2633366X20923671
17. Metal foam web - https://www.metalfoamweb.com/aluminum-foam/closed-cell-aluminum-foam/. Accessed 11 Mar 2022
18. Lopatnikova, S.L., Gamaa, B.A., Haquea, M.J., Krauthausera, C., Gillespie, J.W.: High-velocity plate impact of metal foams. Int. J. Impact Eng. **30**(4), 421–445 (2004)
19. Beals, J.T., Thompson, M.S.: Density gradient effects on aluminium foam compression behavior. J. Materials Sci. **3**(2), 3595–3600 (1997)